Front. Energy 2021, 15(1): 14–25
https://doi.org/10.1007/s11708-020-0805-x

RESEARCH ARTICLE

Yandi ZHANG, Yinhe LIU, Xiaoli DUAN, Yao ZHOU, Xiaoqian LIU, Shijin XU

Effect of temperature on Lu'an bituminous char structure evolution in pyrolysis and combustion

Abstract In the process of pyrolysis and combustion of coal particles, coal structure evolution will be affected by the ash behavior, which will further affect the char reactivity, especially in the ash melting temperature zone. Lu'an bituminous char and ash samples were prepared at the N_2 and air atmospheres respectively across ash melting temperature. A scanning electron microscope (SEM) was used to observe the morphology of char and ash. The specific surface area (SSA) analyzer and thermogravimetric analyzer were respectively adopted to obtain the pore structure characteristics of the coal chars and combustion parameters. Besides, an X-ray diffractometer (XRD) was applied to investigate the graphitization degree of coal chars prepared at different pyrolysis temperatures. The SEM results indicated that the number density and physical dimension of ash spheres exuded from the char particles both gradually increased with the increasing temperature, thus the coalescence of ash spheres could be observed obviously above 1100°C. Some flocculent materials appeared on the surface of the char particles at 1300°C, and it could be speculated that β-Si_3N_4 was generated in the pyrolysis process under N_2. The SSA of the chars decreased with the increasing pyrolysis temperature. Inside the char particles, the micropore area and its proportion in the SSA also declined as the pyrolysis temperature increased. Furthermore, the constantly increasing pyrolysis temperature also caused the reactivity of char decrease, which is consistent with the results obtained by XRD. The higher combustion temperature resulted in the lower porosity and more fragments of the ash.

Received Sept. 6, 2019; accepted Jan. 30, 2020; online Apr. 10, 2020

Yandi ZHANG, Yinhe LIU (✉), Xiaoli DUAN, Yao ZHOU, Xiaoqian LIU, Shijin XU
State Key Laboratory of Multiphase Flow in Power Engineering, Xi'an Jiaotong University, Xi'an 710049, China
E-mail: yinheliu@mail.xjtu.edu.cn

Keywords bituminous char, pyrolysis, ash, structure evolution, reactivity

1 Introduction

Coal, as one of the major fossil energies, greatly supports the global economy development. In the Asian-Pacific region, coal is especially the most reserve-abundant and widely-used fossil energy. According to the data of "BP Statistical Review of World Energy," the coal consumption of Asian-Pacific region in 2018 accounted for 75.3% of its total energy consumption [1]. For a long time to come, coal-fired power generation will still be one of the most mature and effective ways to generate electricity. However, slagging and fouling problems exist in most of coal-fired power plants to varying degrees [2–4]. In detail, slagging is resulted from the deposition of the molten ash on the boiler furnace which is exposed to the flame radiation while fouling is caused by the deposition of the non-molten ash on the lower-temperature convection heating surface [5]. Furthermore, for some slag tapping boilers, whether the char particles could have a stable wall-adherent combustion also relies on the characteristics of the slag [6,7]. The smooth operation and long-term running of the boiler strongly depend on the steady and reliable removal of the slag [8]. In a word, all these issues could be classified as "ash-related problems" [9–13] whose solution greatly depends on the clear cognition of ash fusion behaviors.

In the char-ash/slag transition process, the ash fusion behaviors play an important role. On the one hand, some minerals in the ash can catalyze the conversion of coal char. On the other hand, the molten ash will block some pores and hinder the reaction of carbon. However, it is very difficult to directly obtain the effect of ash fusion behaviors on char characteristics. Therefore, most researchers [14–18] chose the reaction temperature as the index of ash fusion extent and studied the variation of microscopic morphology, specific surface area (SSA) and porosity,

gasification or combustion characteristic indexes, crystalline structure, functional groups etc. with the increase of reaction temperature by scanning electron microscope (SEM), thermogravimetric analyzer (TGA), SSA, X-ray diffractometer (XRD) and Fourier transform infrared spectrometer (FTIR) etc., respectively. Lin et al. [19] proposed that temperature affected char characteristics mainly in the decrease of micropore surface area, incomplete diffusion, ash fusion, and carbon-ash reactions, of which "ash fusion" is the most important. They found that the SSA of the micropores and mesopores of coal char decreased with the increased char-making temperature, because the molten ash could easily cover the micropores and mesopores, while the SSA of macropores hardly varied for the fact that the whole volume of ash is far less than that of the macropores, thus ash fusion had little effect on the SSA of macropores. Ding et al. [20] also agreed with the fact that ash fusion temperature was a very important parameter during the gasification process, and they obtained the threshold value of gasification conversion (x = 0.9) for Yunnan lignite and Shenfu bituminous when the gasification temperature was higher than the ash fusion temperature. Wu et al. [21] studied the effect of ash fusion on the gasification reactivity and found that the molten ash would adhere to the surface of the char, which restricted the further gasification reaction. Liu et al. [22] found that the SSA of char particles with a lower ash fusion point decreased with the pyrolysis temperature increasing and ash accumulation was observed, but this variation was opposite and no accumulation significance existed for char particles with a higher ash fusion point. However, the variation of ash behaviors in char across ash melting temperature zone, the effect of different ash fusion extent on the porosity structure, and the reactivity of char are still not clear. Thus, further experimental research should be conducted with the help of SEM-energy dispersive spectrometer (SEM-EDS) to clearly observe the exudation and accumulation of ash spheres, by which the results of SSA and TGA of char with char-making temperature increasing could be deeply understood.

Variable ash fusion behaviors of the char prepared in different pyrolysis temperatures give rise to the difference of the char micro structure, accordingly the combustion reactivity of coal chars are different [23]. Tang et al. [24] found that the rising pyrolysis temperature would lead to the increase of ignition temperature (IT) and $t_{0.5}$ which referred to the corresponding temperature of 50% weight loss of the fixed carbon, meanwhile the char reactivity declined in this process. Wang et al. [25] studied the pyrolysis characteristics of rice straw, coke and coal, whose results showed that both the ignition and burn-out points would be delayed with the pyrolysis temperature rising, and the combustion reactivity would decline as well, while the pyrolysis temperature had no obvious effect on the char reactivity of rice straw. Most researchers mainly focus on the interaction between preparing temperatures and reactivity of the coal char; however, the char structure characteristics including the SSA and their effects on char reactivity are also the key issues of the reaction kinetics.

Bituminous coal, as the most important, widespread, and abundant coal in the world [26], is often used primarily as fuel in steam-electric power generation [27]. In this paper, Lu'an bituminous coal was studied and the char particles were prepared on a fixed bed reactor in N_2 atmosphere at different temperatures across the ash melting temperature zone, and the SEM, SSA analyzer, TGA and XRD were used to obtain the micro morphology, SSA, combustion characteristic parameters and graphitization degree. Besides, the ash prepared under air atmosphere at different temperatures was also observed by SEM to get the effect of combustion temperature on ash particles. With those analyses, the ash fusion behaviors on coal char characteristics in the pyrolysis and combustion process could be further understood, which provides a theoretical basis for the solution of ash-related problems in the operation of coal fired power plants.

2 Experiment

2.1 Coal sample

Lu'an bituminous coal was used in the present study due to its huge reserves in Shanxi Province, China. Lu'an coal was air-dried at 105°C, milled and sieved to a size of 91–125 μm. Table 1 shows the proximate analysis, ultimate analysis (5E-MAG6600 analyzer, China), and ash fusion characteristics (HR-8 ash fusion point meter, China) of Lu'an bituminous coal and ash. The ash composition as shown in Table 2 was analyzed by using the semi micro chemical analysis method and the atomic absorption method according to Chinese Standard GB/T1547-2007.

2.2 Experimental device and procedure

Char and ash samples were prepared on the experimental device as shown in Fig. 1. The furnace was heated by

Table 1 Analyses of Lu'an bituminous coal and ash (air-dried basis)

Proximate analysis/wt%				Ultimate analysis/wt%					Ash fusion temperature t/°C			
M_{ad}	A_{ad}	V_{ad}	FC_{ad}	C_{ad}	H_{ad}	N_{ad}	S_{ad}	O_{ad}*	DT	ST	HT	FT
6.83	10.92	31.78	50.47	61.35	2.97	0.57	0.14	17.22	1140	1180	1190	1200

Notes: M—moisture; A—ash; V—volatile; FC—fixed carbon; ad—air-dried; DT—deformation temperature; ST—softening temperature; HT—hemispherical temperature; FT—flow temperature. *Calculated by difference.

Table 2 Ash composition analysis of Lu'an bituminous coal

Ash composition	SiO_2	Al_2O_3	Fe_2O_3	CaO	MgO	Na_2O	K_2O	TiO_2	SO_3
Content/wt%	36.75	16.32	6.46	27.54	2.74	2.90	0.24	0.94	3.70

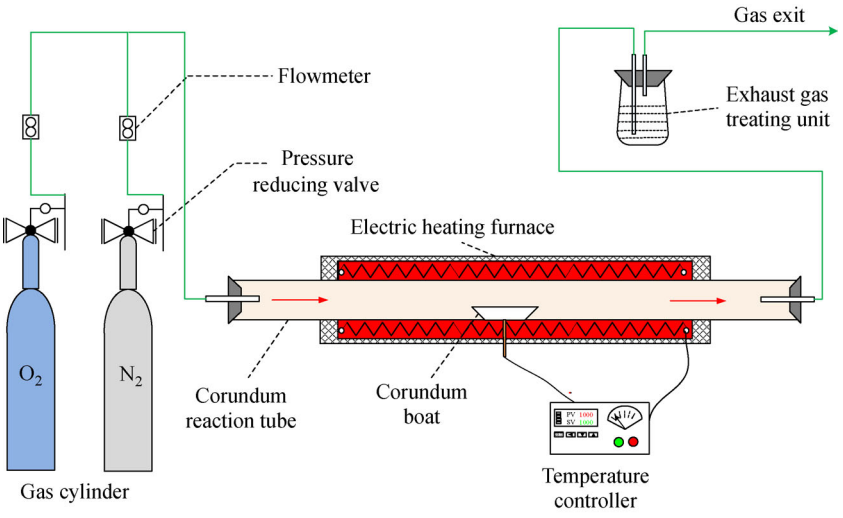

Fig. 1 Experimental setup of fixed bed for bituminous char/ash preparing.

electric heating components and controlled by a temperature-programmed controller. Two mass flow controllers were used to regulate the flowrate of N_2 and O_2. First, the empty furnace was pre-heated to a preset temperature and the specified gas was injected beforehand to expel the air in the reaction tube with a total flow rate of 1 L/min. About 1.5 g of parent Lu'an coal was paved uniformly at the bottom of the corundum boat with a thickness of 1 mm. The corundum boat was put into the preparing section for preheating, and then moved to the heating section which was preheated to the reaction temperature at the set heating rate, and finally pushed to the cooling section after pyrolysis and combustion. The heating temperature was in the range of 900°C to 1300°C at the interval of 100°C, according to the ash fusion temperature. The residence time was 1 h in pure N_2 for char preparing and 40 min in 79%N_2/21%O_2 for ash preparing.

2.3 Analysis methods

The coal char and ash samples prepared were analyzed by the SEM-EDS and SSA analyzer, while the varieties of combustion reactivity and the graphitization degree of coal chars with pyrolysis temperature were respectively studied by TGA and XRD.

2.3.1 SEM-EDS analysis

A field emission SEM (SEM JSM-6390A, Japan) equipped with an EDS manufactured by JEOL Ltd. was used to observe the surface morphology of char/ash samples by operating SEM at an accelerating voltage of 15 kV, beam spot size of 40 nm, and working distance of 10 mm in *Z* direction. EDS was used for the qualitative element identification and semiquantitative elemental analysis at the selected local area of char/ash samples surface.

2.3.2 SSA analysis

A Rise-1010 automatic SSA analyzer was used to measure the SSA and micropore area of samples through the low temperature nitrogen physical adsorption. The Rise-1010 had a high precision for the porous sample whose SSA is larger than 0.001 m^2/g.

2.3.3 Thermogravimetric analysis

A SETARAM Labsys Evo simultaneous thermogravimetric analyzer made in France was used to characterize the reactivity of char samples. A thermogravimetric analysis was performed under non-isothermal conditions with a heating rate of 10°C /min from ambient temperature to 1200°C. The char sample (10.0±0.1 mg) was used in each run in 15%O_2/85%N_2 flow of 60 mL/min. The combustion characteristics parameters of char were obtained by TG/DTG curves to reveal the change of char reactivity.

2.3.4 X-ray diffraction analysis

The XRD was occupied to give the carbon crystalline structure of coal char prepared at different temperatures.

X-ray diffraction patterns was recorded on an X'pert Pro XRD operating at 40 kV and 40 mA with Cu Kα radiation over 10°–90° with a wavelength of 1.5406 Angstrom. The scanning speed and step size are 4°/min and 0.02°, respectively.

3 Results and discussion

3.1 Effect of pyrolysis temperature on char structure evolution

3.1.1 Effect of pyrolysis temperature on micro-morphology of bituminous char

Temperature is one of the controlling factors for coal conversion, which influences the variation of crystallite structure and the evolution process of the structure, such as the sintering and ash melting process of char. Figure 2 demonstrates the char yield of Lu'an bituminous coal at different pyrolysis temperatures. The char yield decreases gradually with the increasing pyrolysis temperature, but decreases sharply in the range of 1200°C–1300°C, which may be related to the decomposition reaction of sulfate minerals in char [15]. To investigate the exudation and coalescence of ash in char evolution process across ash melting temperature zone, the char prepared at different temperatures were observed by the SEM. The micro-morphology of parent coal and chars prepared in N_2 are depicted in Fig. 3.

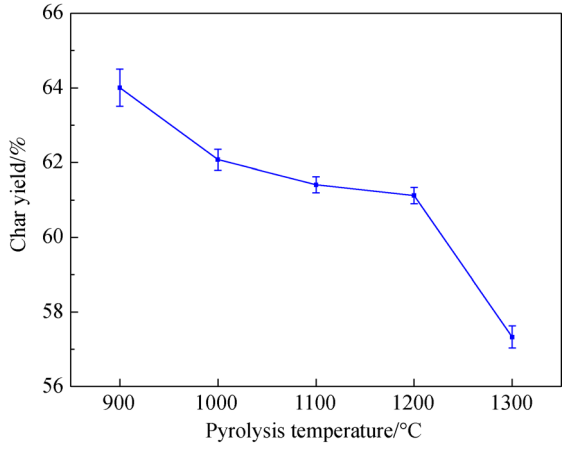

Fig. 2 Char yield of Lu'an bituminous coal at different pyrolysis temperatures.

The sizes of the chars produced are almost the same as that of parent coal in Fig. 3, which suggests that Lu'an bituminous coal has a high thermal stability and the fragmentation does not occur in the heating process of the particles. However, the brightness of char particles increases significantly compared to that of parent coal. To understand this phenomenon, the char was observed with the SEM under high magnification, whose results are exhibited in Fig. 4.

The highlight areas marked with squares in Fig. 4 exist in all the char particles prepared at different pyrolysis temperatures. The dense arrangement of the highlight areas results in higher brightness of the char than that of the coal particles in the SEM horizon. Taking the char prepared at 900°C for example, qualitative analysis was performed on the element composition of none-highlight area (hexagon area 001) and highlight area (square area 002) by the EDS, whose results are given in Table 3, in which the errors of mineral element measurement meet the Chinese Standard of GB/T17359-1998. The content of mineral elements, such as Mg, Ca, Fe etc., are apparently higher than that of the none-highlight area. The elements above mentioned mainly exist in the mineral of the char, which would transform into ash under high-temperature thermal treatment. Both the higher hardness and larger average atomic number lead to the higher brightness of the secondary electron image than that of the organic macerals [28]. Thus, the higher content of ash on the surface of the coal char results in the emergence of the highlight area in Fig. 4.

In the heating process of coal char across the ash melting temperature, the ash with different fusion points successively exudes on the surface of the char through the pore channel and forms ash spheres one after the other. As displayed in Fig. 4, when the pyrolysis temperature is 900°C, fixed carbon account for a huge share on the surface of coal char while the content of highlighted ash is much less. The shape of the ash is still irregular. When the pyrolysis temperature rises to 1000°C, some ash spheres appear on the surface of the coal char. Compared with the ash at 900°C, the number density of the ash spheres in char is obviously higher while the enlargement of the physical dimension is not evident. When the pyrolysis temperature increases to 1100°C, a large number of ash spheres with larger particle sizes could be observed by the SEM. As the pyrolysis temperature further increases, both the density and physical dimension of the ash spheres exuded from the char gradually increase. Meanwhile, the difference of physical dimension between different ash spheres is gradually growing. When the pyrolysis temperature rises to 1300°C, the fusion phenomenon of the ash exuded from the coal char appears and the adjacent ash spheres coalesce to form larger ash pellets.

Besides, it can be seen from Fig. 3(f) that some flocculent substance emerged on the surface of coal char in the SEM horizon. To clearly observe these flocculent substances, the magnification times of 200, 2000, and 5000 of SEM were employed and the results are presented in Fig. 5.

As can be observed in Fig. 5, the needle-like materials form a dense net structure in the way of crossover and conglutination. To find out the specific components of the needle-like materials, the EDS was employed on the needle-like materials abundant zone (003) and needle-like

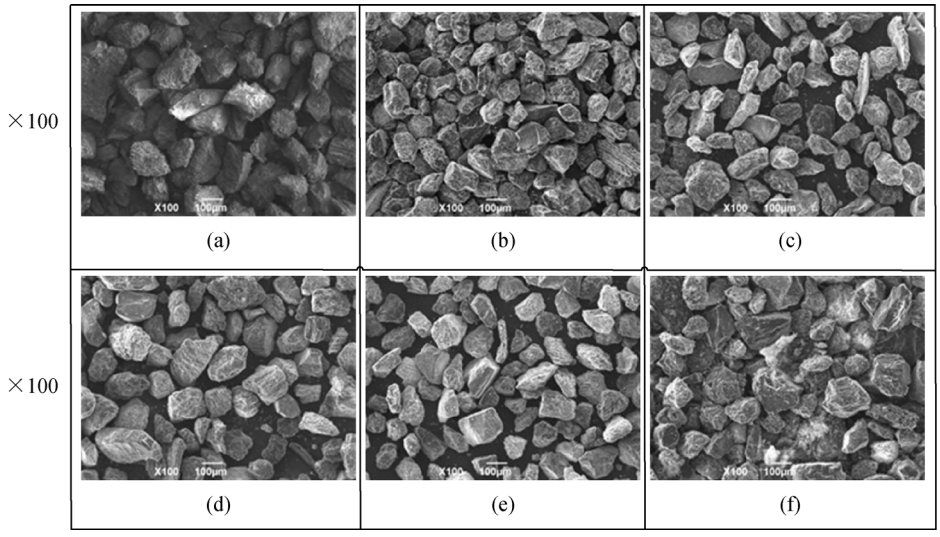

Fig. 3 Micro-morphology of parent coal and char.
(a) Raw coal; (b) char prepared at 900°C; (c) char prepared at 1000°C; (d) char prepared at 1100°C; (e) char prepared at 1200°C; (f) char prepared at 1300°C.

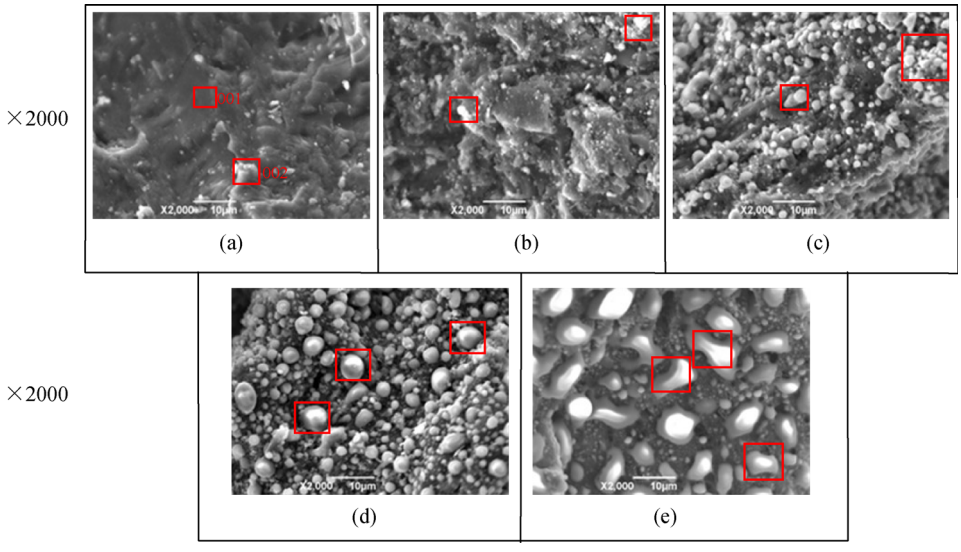

Fig. 4 Effect of pyrolysis temperature on char behavior.
(a) Char prepared at 900°C; (b) char prepared at 1000°C; (c) char prepared at 1100°C; (d) char prepared at 1200°C; (e) char prepared at 1300°C.

materials non-abundant zones (004 and 005), and the results are listed in Table 4.

Table 4 shows that the mass percentage of N and Si elements in needle-like materials abundant zone (003) in Fig. 4 are as high as 17.13% and 54.77%, respectively, while the mass percentage of C element is only 23.74%. However, the mass percentages of C element in the non-abundant zones (004 and 005) of needle-like materials are both higher than 70%, while the content of N and Si elements are much lower than that in the abundant zone (003) of needle-like materials, especially for N element, which is rarely subsistent according to the EDS results. Therefore, the elements of N and Si should be responsible for the emergence of needle-like materials.

As previously mentioned, the element content of N_{ad} in Lu'an bituminous char is only 0.58%. Therefore, it can be speculated that such a huge N content must be derived from the inert pyrolysis N_2 atmosphere. For this reason, the C and SiO_2 of coal char might react with the N_2 of pyrolysis atmosphere under certain high temperature conditions. The reaction equation might be

$$3SiO_2 + 6C + 2N_2 \rightarrow Si_3N_4 + 6CO \quad (1)$$

Table 3 EDS analysis of non-highlighted area (001) and highlighted area (002)

Elements	Mass percentage of element/%	
	Non-highlighted area (001)	Highlighted area (002)
C	64.96±2.53	28.85±0.81
O	10.31±1.85	32.37±0.69
Mg	0	1.04±0.08
Al	1.79±0.36	1.56±0.09
Si	12.53±1	11.56±0.24
Ca	8.99±1.14	23.34±0.42
Fe	0	1.01±0.23

There are two types of Si_3N_4 crystals [29], one type being α-Si_3N_4 and the other being β-Si_3N_4, which are granular and needle-like in microcosmic view, respectively. According to the characteristics of the Si_3N_4 crystal in the experiment, this needle-like material should be β-Si_3N_4. To verify this speculation, the thermodynamic equilibrium software—FactSage was employed to calculate the results of 6 mol C and 3 mol SiO_2 in 2 mol N_2 atmosphere, whose results are shown in Fig. 6.

The results of FactSage indicated that Si_3N_4 and CO were generated in this reaction. As the pyrolysis temperature rose, the Gibbs free energy (ΔG) decreased linearly, which was consistent with the result that the chemical equilibrium gradually shifted toward the generation of Si_3N_4. When the pyrolysis temperature was 1200°C, the quantity of Si_3N_4 produced from the above reaction was merely 0.0296 mol. However, when the pyrolysis temperature increased to 1300°C, the quantity of

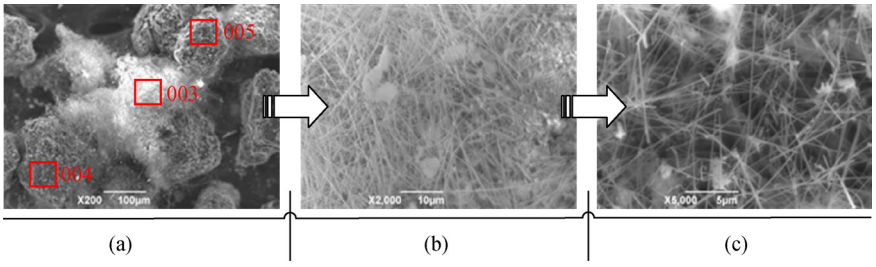

Fig. 5 SEM analysis of flocculent substance.
(a) × 200; (b) × 2000; (c) × 5000.

Table 4 EDS analyses on needle-like materials abundant zone (003) and needle-like materials non-abundant zones (004 and 005)

Elements	Mass percentage of element/%		
	Needle-like materials abundant zone (003)	Needle-like materials non-abundant zone (004)	Needle-like materials non-abundant zone (005)
C	23.74±0.28	75.52±0.23	83.65±0.25
N	17.13±0.82	0	0
O	1.66±0.38	3.29±0.98	4.35±1.69
Al	0.99±0.12	0.74±0.29	0.49±0.49
Si	54.77±0.14	18.19±0.32	10.18±0.54
Ca	1.24±0.36	1.54±0.77	0.98±1.26

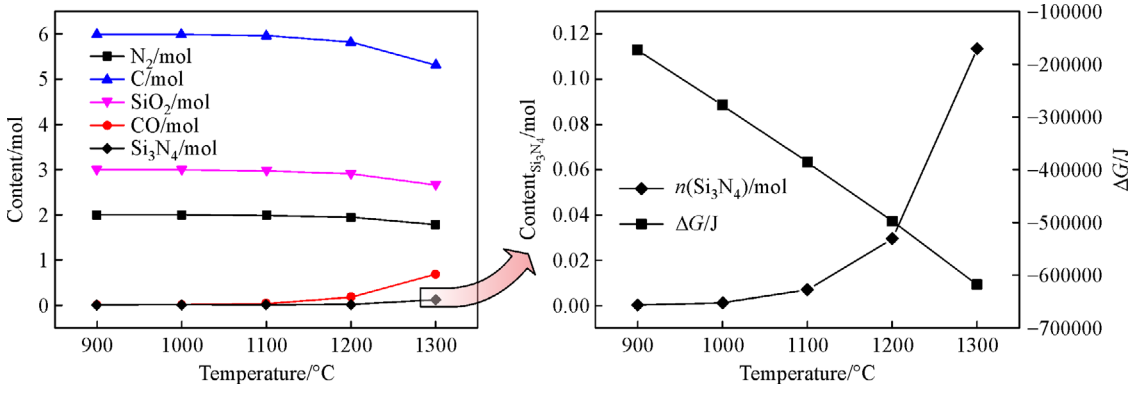

Fig. 6 Reaction of C and SiO_2 in N_2 atmosphere at different temperatures.

Si_3N_4 rapidly rose to 0.114 mol, nearly three times higher than that of 1200°C. The results could well explain the reason for the emergence of plenty of needle-like materials in 1300°C in N_2 atmosphere.

To further verify whether the formation of needle-like substance was caused by the N_2 of the pyrolysis atmosphere, the Ar atmosphere was used to replace the N_2 atmosphere on original fixed bed experimental setup to obtain the coal char in 1300°C. Figure 7 exhibits the SEM images of the coal char prepared in Ar atmosphere at 1300°C.

As shown in Fig. 7, when the pyrolysis temperature was 1300°C, the surface morphology of coal char prepared in N_2 and Ar atmosphere was basically similar, except the fact that none needle-like materials were generated on the surface of the char particles prepared in Ar atmosphere. Therefore, the needle-like materials are further verified to be Si_3N_4 crystal.

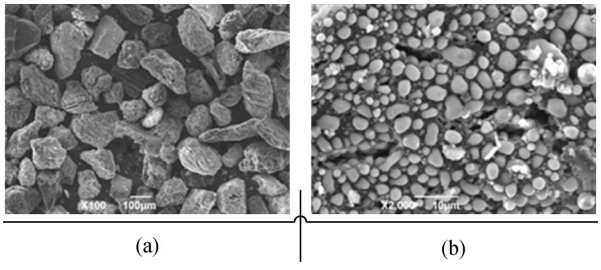

Fig. 7 SEM images of coal char prepared in Ar atmosphere. (a) × 100; (b) × 2000.

3.1.2 Effect of pyrolysis temperature on SSA of bituminous char

The SSA and pore diameter are two important parameters of coal char in its structure evolution process. Understanding the variation mechanism of the two parameters abovementioned has a great significance in describing the reactivity of char and obtaining the combustion rate [30]. Many researchers [31–34] have studied the pore size classification for many years. Based on the physical adsorption capability and capillary condensation theory [35], the International Union of Pure and Applied Chemistry (IUPAC) divided the pores into three categories: micropores ($d < 2$ nm), mesopores (d = 2–50 nm), and macropores ($d > 50$ nm) [36].

The Rise-1010 SSA analyzer was used to measure the SSA and micropore area (MIA) of the coal char prepared in the pyrolysis process at different temperatures across the ash melting temperature zone. Then, by using Eqs. (2)–(4), the percentage of the micropore area (PMIA), the sum of the mesopore area and the macropore area (MEA&MAA), and the sum percentage of the mesopore area and the macropore area (PMEA&PMAA) of the coal char are respectively figured out to clarify the variation mechanism of SSA and the pore structure of coal char with pyrolysis temperature increasing. Figure 8 gives the effect of pyrolysis temperature on SSA of char particles in N_2 atmosphere while Figs. 9 and 10 respectively show the variation of MIA, MEA&MAA, and their percentage accounting for the SSA as pyrolysis temperature increasing.

$$\mathrm{PMIA} = \frac{\mathrm{MIA}}{\mathrm{SSA}} \times 100\%, \tag{2}$$

$$\mathrm{MEA{+}MAA} = \mathrm{SSA} - \mathrm{MIA}, \tag{3}$$

$$\begin{aligned} \mathrm{PEMA} + \mathrm{PMAA} &= \frac{\mathrm{MEA} + \mathrm{MAA}}{\mathrm{SSA}} \times 100\% \\ &= 1 - \mathrm{PMIA}. \end{aligned} \tag{4}$$

The SSA of coal char decreases with pyrolysis temperature increasing across ash melting temperature zone in Fig. 8. When the pyrolysis temperature is 900°C, the SSA of coal char is 188.25 m^2/g; but when the pyrolysis temperature rises to 1300°C, the SSA of coal char decreases to 42.44 m^2/g. The SSA variation of coal char could mainly be caused by the transformation of pore structure, especially for micropores, which are very difficult to be directly observed by the SEM, thus the gas adsorption method is a feasible and accurate way to measure the micropores of the char to speculate the pore structure evolution in the pyrolysis process. Seen from Fig. 9, both the MIA and MEA&MAA decrease with the pyrolysis temperature increasing, which collectively leads to the decline of the SSA of coal char, just as Fig. 8 shown. Besides, the variation range of MIA is much larger than that of MEA&MAA, which demonstrates that in the pyrolysis process of coal char across the ash melting temperature zone, the sharp decline of the micropore area is the dominant factor for the decrease of the SSA of coal char. Meanwhile, combining with the results of Fig. 10, it is easy to see that with the pyrolysis temperature rising, PMIA is gradually decreasing while the tendency of

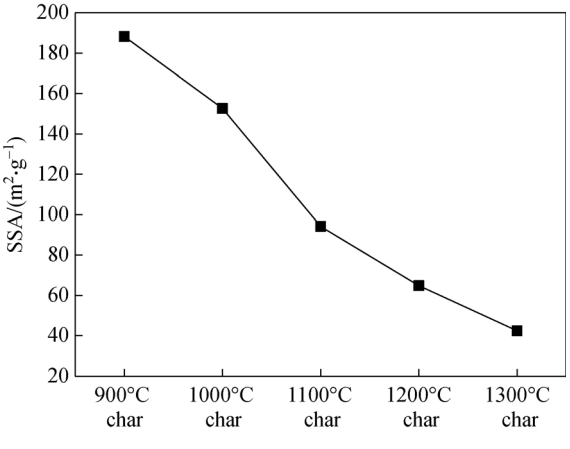

Fig. 8 Effect of pyrolysis temperature on SSA of coal char.

PMEA&PMAA is just opposite. Connecting with the SEM images in Section 3.1.1, it is reasonable to infer the evolution of the pore structure in the pyrolysis process: with the increase of pyrolysis temperature, the micropores of coal char continuously collapse or coalesce. As a result, numerous micropores on the one hand might be filled or covered by the molten ash; on the other hand, some of the micropores transform into mesopore or macropore, which leads to the increase in the average pore diameter. All abovementioned factors contribute to the variation of the SSA and pore structure evolution of coal char in the pyrolysis process.

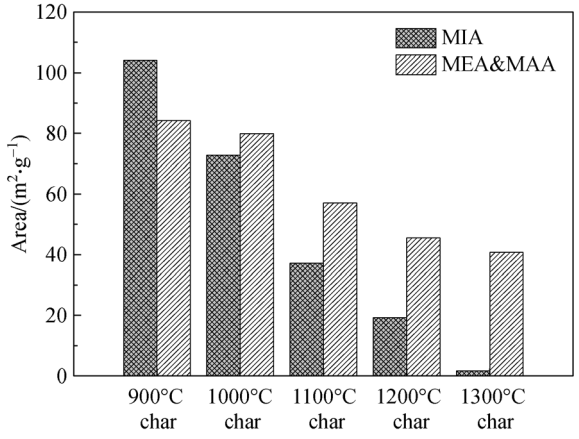

Fig. 9 Effect of pyrolysis temperature on MIA and MEA&MAA of coal char.

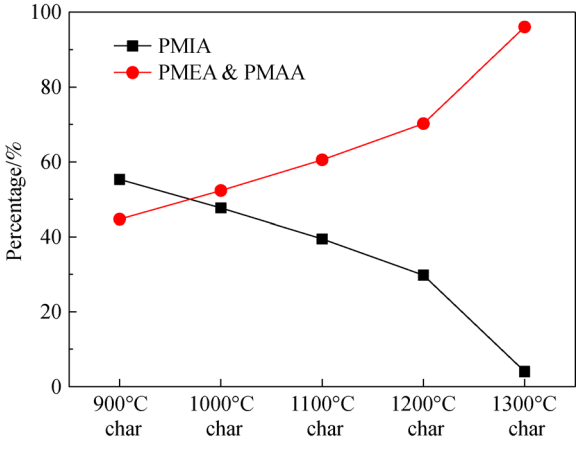

Fig. 10 Effect of pyrolysis temperature on PMIA and PMEA& PMAA of coal char.

3.1.3 Effect of pyrolysis temperature on combustion reactivity of bituminous char

Both the SSA and pore structure of char at a high temperature influence the reactivity and combustion rate of char [30]. To obtain the combustion reactivity of coal char with the pyrolysis temperatures across ash melting temperature, a thermogravimetric analysis was performed on a LabsysEvo simultaneous thermal analyzer. Figure 11 shows the TG and DTG curves. The tangential line method [37,38] was used to obtain the IT and the burnout temperature (BT) of char. The ignition temperatures (ITs) and burnout temperatures (BTs) of coal char prepared at different pyrolysis temperatures are exhibited in Fig. 12.

As can be noticed in Fig. 12, the ITs and BTs of char increase with pyrolysis temperature increasing. The ignition and burnout of char postpone for high temperature pyrolysis. One reason for this is that as the pyrolysis temperature increases, the ordering of the char crystallinity increases. The other reason is that SSA is also an important factor; the char with a higher SSA has a lower IT. This IT trend is consistent with the SSA results in Fig. 8.

Many scholars [39–41] applied XRD to analyze the microcrystalline structure characteristics of coal char and correlated the reactivity of coal char with the crystallite structure parameters. The interplanar spacing d_{002} and the graphitization degree G of the carbon crystallites are calculated according to the Bragg equation [40] and the Mering-Maire formula [42], and are defined as Eqs. (5) and (6), respectively.

$$d_{002} = \frac{\lambda}{2\sin\theta_{002}}, \tag{5}$$

$$G = \frac{0.3440 - d_{002}}{0.3440 - 0.3354} \times 100\%, \tag{6}$$

where d_{002} is the interplanar distance of the carbon (002) plane, θ_{002} is the half angle of the diffraction angle of the corresponding 002 peak on XRD, λ is the X-ray diffraction wavelength, G is the graphitization degree, 0.3440 is the completely non-graphitized interplanar distance of carbon, and 0.3354 is the interplanar distance of the ideal graphite crystal. The larger capitalized G means the higher degree of graphitization of the coal char, which then leads to the decreasing of the reactivity. Table 5 listed the interplanar distance d_{002} and graphitization degree G of chars prepared at different pyrolysis temperatures.

As can be noticed in Table 5, with the increasing of pyrolysis temperature, the interplanar distance d_{002} of coal char crystallites decreases, the coal microcrystal structure steadily develops orderly, the graphitization degree G gradually increases, and the combustion reactivity of coal char decreases. This is consistent with the change of the IT and BT of coal char particles with the pyrolysis temperature. Considering the pore structure evolution abovementioned, it can be concluded that part of the micropore will collapse, coalescence, or be blocked by the exuded molten ash inside or at the entrance of pore at high pyrolysis temperature, which will result in the decrease of

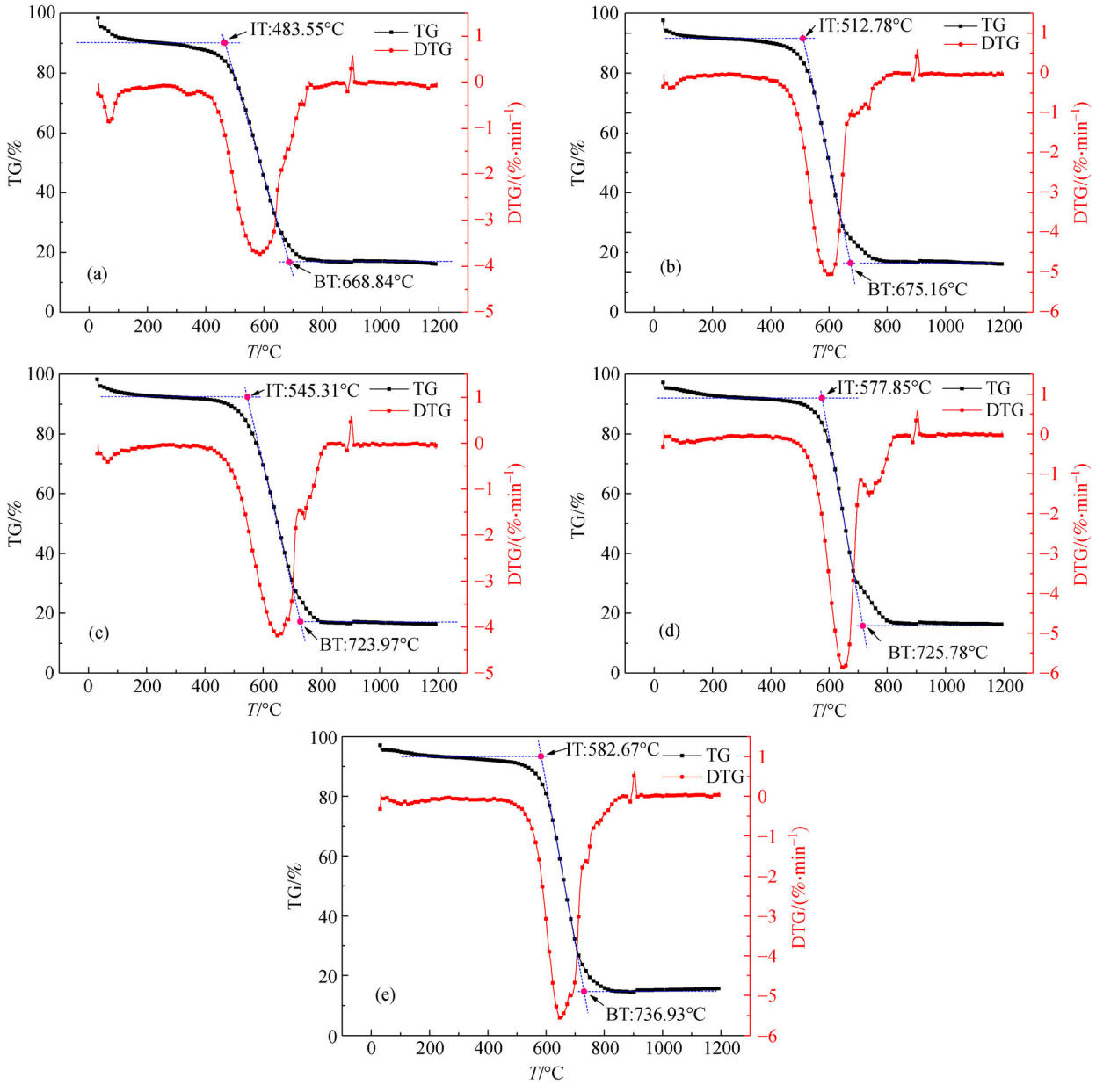

Fig. 11 TG/DTG curves of char prepared at different temperatures.
(a) 900°C; (b) 1000°C; (c) 1100°C; (d) 1200°C; (e) 1300°C.

micropore area and the decrease of total surface area of char particle. Therefore, the reactivity of char varies with the pyrolysis temperature.

3.2 Effect of combustion temperature on micro-morphology of bituminous char

Coal particles undergo a series of complex processes including devolatilization, carbon polycondensation, and ash sintering and melting when entering the furnace in the air atmosphere (79% N_2/21% O_2). The combustion temperature is an important factor affecting the ash morphology. To obtain the effect of combustion temperature on coal char structure evolution across ash melting point, the ash samples were prepared on the fixed bed under 79% N_2/21% O_2 at different temperatures and observed by the SEM. From Table 1, it can be seen that the FT of the ash of Lu'an coal is 1200°C. The coal ash sticks to the bottom of the corundum crucible due to the ash fusion. Therefore, the microstructure of the ash cannot be observed by the SEM when combustion temperature is over 1200°C. The microscopic images of the samples of coal ash prepared at 900°C–1100°C for 40 min in air atmosphere are given in Fig. 13.

The SEM images with the magnification of 100 times in Fig. 13 show that the average size of coal ash particles

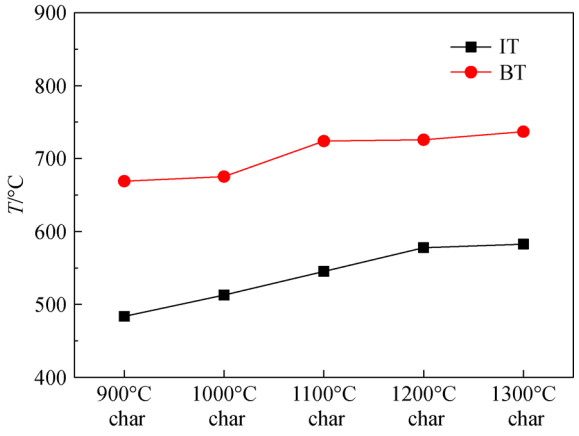

Fig. 12 ITs and BTs of coal char at different pyrolysis temperatures.

shrinks as the combustion temperature increases. The shrinkage in rice straw char was also observed by Ding et al. in the *in situ* heating stage [43]. With the intention of getting a more detailed morphology, the ash particles were observed by the SEM at a magnitude of 2000 times. The pore structure was well developed when combustion temperature rose to 900°C. When combustion temperature increased to 1000°C, the initial softening and deformation of coal ashes could be observed under the SEM, with the gradually rounding of ash sharp edge or tip and the decrease of porosity. Thus, it is reasonable to speculate that the collapse and combination of ash pores occur. When the combustion temperature rose to 1100°C, the particles began melting obviously, less pores were observed at a magnitude of 2000 times SEM and the particle tended to be round and dense, which may account for the fact that the size of ash particle decreases with increasing combustion temperature.

4 Conclusions

In this paper, the effect of temperature on Lu'an bituminous coal in pyrolysis and combustion was investigated. Limited by the experimental conditions, only Lu'an bituminous coal was selected, while different ash compositions and changes in coal quality might also affect the structure evolution behavior of bituminous coal char. Therefore, it is necessary to expand the experimental coal and conduct further research. The morphology of char prepared in N_2 and ash prepared in air atmosphere across ash melting temperature were observed by using the SEM-EDS. The SSA and TGA were used to obtain the porosity and combustion kinetics of char combustion. XRD was performed to get the graphitization degree of char. The conclusions are drawn as follows:

The number density and physical dimension of ash spheres exuded on the surface of char particles increase

Table 5 Comparison of combustion reactivity of coal chars prepared at different pyrolysis temperatures

Pyrolysis temperature/°C	900	1000	1100	1200	1300
d_{002}/nm	0.34205	0.3411	0.34048	0.33968	0.33899
G/%	22.67	33.72	40.93	50.23	58.26

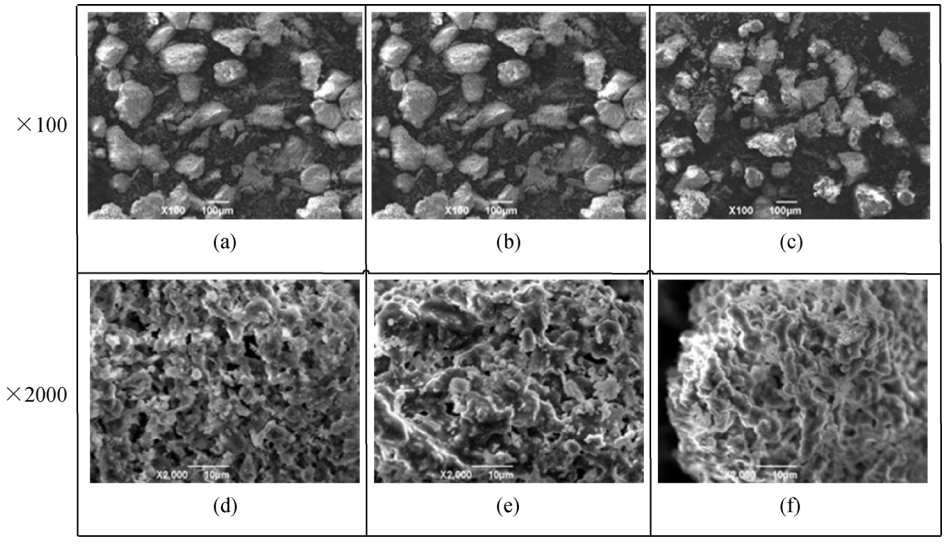

Fig. 13 Morphology of coal ash at various combustion temperatures.
(a) Char prepared at 900°C (× 100); (b) char prepared at 1000°C (× 100); (c) char prepared at 1100°C (× 100); (d) char prepared at 900°C (× 2000); (e) char prepared at 1000°C (× 2000); (f) char prepared at 1100°C (× 2000).

gradually, and the coalescence behavior of the ash spheres can be observed more frequently and obviously with the increase of pyrolysis temperature. The flocculent materials on the surface of the char are formed by the mutual adhesion of the needle-like materials at the pyrolysis temperature of 1300°C. It is speculated that the coal particles formed β-Si_3N_4 in N_2 atmosphere.

The increase of pyrolysis temperature directly leads to the SSA decrease of coal char, meanwhile the micropore area and its proportion in SSA of coal char also continuously declines. The sum area of mesopore and macropore also decreases, while their proportion appears to have the opposite tendency compared with the micropores. The collapse or coalescence of the micropores in coal char might occur, resulting in the fact that plenty of micropores in char transform into mesopores or even macropores.

The increasing pyrolysis temperature results in the increase of the ITs and BTs of the char combustion reaction, with the apparent activation energy and the graphitization degree *G* rising, both of which represent the reactivity decline of char.

With the increase of combustion temperature, the particles tend to be compact, which can be obviously reflect from the decrease of the particle size and the porosity of the coal ash particles.

Acknowledgements This work was financial supported by the National Natural Science Foundation of China (Grant No. 51576158).

References

1. BP. BP Statistical Review of World Energy, 2019, 45
2. Teixeira P, Lopes H, Gulyurtlu I, Lapa N, Abelha P. Evaluation of slagging and fouling tendency during biomass co-firing with coal in a fluidized bed. Biomass and Bioenergy, 2012, 39: 192–203
3. Williams A. Understanding slagging and fouling during PF combustion: Gordon Couch IEA Coal Research. Fuel, 1995, 74 (10): 1541
4. Benson S A, Harb J N. Fuel minerals, fouling and slagging. Energy & Fuels, 1993, 7(6): 743–745
5. Seggiani M. Empirical correlations of the ash fusion temperatures and temperature of critical viscosity for coal and biomass ashes. Fuel, 1999, 78(9): 1121–1125
6. Noda R, Naruse I, Ohtake K. Fundamentals on combustion and gasification behavior of coal particle trapped on molten slag layer. Journal of Chemical Engineering of Japan, 1996, 29(2): 235–241
7. Wang X, Zhao D, He L, Chen Y, Aoki H, Miura T. Study on the mechanism and simulation method for wall burning process. Chinese Journal of Theoretical and Applied Mechanics, 2006, 38(4): 462–470
8. Kong L, Bai J, Li W, Wen X, Liu X, Li X, Bai Z, Guo Z, Li H. The internal and external factor on coal ash slag viscosity at high temperatures, part 2: effect of residual carbon on slag viscosity. Fuel, 2015, 158: 976–982
9. Ma Z, Iman F, Lu P, Sears R, Kong L, Rokanuzzaman A S, McCollor D P, Benson S A. A comprehensive slagging and fouling prediction tool for coal-fired boilers and its validation/application. Fuel Processing Technology, 2007, 88(11–12): 1035–1043
10. Lackner M, Winter F, Agarwal A K. Handbook of Combustion, Vol. 4: Solid Fuels. Weinheim, Germany: Wiley-VCH Verlag GmbH & Co. KGaA, 2010, 493–531
11. Fryda L, Sobrino C, Cieplik M, van de Kamp W L. Study on ash deposition under oxyfuel combustion of coal/biomass blends. Fuel, 2010, 89(8): 1889–1902
12. Akiyama K, Pak H, Tada T, Ueki Y, Yoshiie R, Naruse I. Ash deposition behavior of upgraded brown coal and bituminous coal. Energy & Fuels, 2010, 24(8): 4138–4143
13. Wu X, Ji H, Dai B, Zhang L. Xinjiang lignite ash slagging and flowability under the weak reducing environment at 1300°C—a new method to quantify slag flow velocity and its correlation with slag properties. Fuel Processing Technology, 2018, 171: 173–182
14. Dai B, Hoadley A, Zhang L. Characteristics of high temperature C–CO_2 gasification reactivity of Victorian brown coal char and its blends with high ash fusion temperature bituminous coal. Fuel, 2017, 202: 352–365
15. Ma Z, Bai J, Li W, Bai Z, Kong L. Mineral transformation in char and its effect on coal char gasification reactivity at high temperatures, part 1: mineral transformation in char. Energy & Fuels, 2013, 27(8): 4545–4554
16. Ma Z, Bai J, Bai Z, Kong L, Guo Z, Yan J, Li W. Mineral transformation in char and its effect on coal char gasification reactivity at high temperatures, part 2: char gasification. Energy & Fuels, 2014, 28(3): 1846–1853
17. Bai J, Li W, Li C, Bai Z, Li B. Influences of minerals transformation on the reactivity of high temperature char gasification. Fuel Processing Technology, 2010, 91(4): 404–409
18. Ma Z, Bai J, Wen X, Li X, Shi Y, Bai Z, Kong L, Guo Z, Yan J, Li W. Mineral transformation in char and its effect on coal char gasification reactivity at high temperatures part 3: carbon thermal reaction. Energy & Fuels, 2014, 28(5): 3066–3073
19. Lin S Y, Hirato M, Horio M. The characteristics of coal char gasification at around ash melting temperature. Energy & Fuels, 1994, 8(3): 598–606
20. Ding L, Zhou Z, Guo Q, Wang Y, Yu G. *In situ* analysis and mechanism study of char-ash/slag transition in pulverized coal gasification. Energy & Fuels, 2015, 29(6): 3532–3544
21. Wu X, Zhang Z, Piao G, He X, Chen Y, Kobayashi N, Mori S, Itaya Y. Behavior of mineral matters in Chinese coal ash melting during char-CO_2 /H_2O gasification reaction. Energy & Fuels, 2009, 23(5): 2420–2428
22. Liu H, Luo C, Toyota M, Uemiya S, Kojima T. Kinetics of CO_2/char gasification at elevated temperatures. Part II: clarification of mechanism through modelling and char characterization. Fuel Processing Technology, 2006, 87(9): 769–774
23. Shen C, Lin W, Wu S, Tong X, Song W. Experimental study of combustion characteristics of bituminous char derived under mild pyrolysis conditions. Energy & Fuels, 2009, 23(11): 5322–5330
24. Tang L, Hu S, Ni Y, Zhu X, Zhu Z. Effect of char marking temperature on coal char characteristics. Journal of East China

University of Science and Technology, 2007, 33(2): 149–152
25. Wang X, Xu W, Zhang L, Hu Z, Tan H, Xiong Y, Xu T. Char characteristics from the pyrolysis of straw, wood and coal at high temperatures. Journal of Biobased Materials and Bioenergy, 2013, 7(6): 675–683
26. Xie K. Coal Structure and its Reactivity. Beijing: Science Press, 2002
27. Speight J G. Handbook of Coal Analysis. 2nd ed. Hoboken: John Wiley & Sons, Inc, 2015
28. Zhang H, Li X. Application of scanning electron microscope in coal and rock science. Journal of Chinese Electron Microscopy Society, 2004, 23(4): 467–467
29. Cao J, Cong L. Discussion on the research and application of silicon nitride. Ceramics, 2008, 4(8): 34–36
30. Lorenz H, Carrea E, Tamura M, Haas J. The role of char surface structure development in pulverized fuel combustion. Fuel, 2000, 79(10): 1161–1172
31. Shi J Q, Durucan S. Gas storage and flow in coalbed reservoirs: implementation of a bidisperse pore model for gas diffusion in coal matrix. SPE Reservoir Evaluation & Engineering, 2005, 8(02): 169–175
32. Clarkson C R, Wood J, Burgis S, Aquino S, Freeman M. Nanopore-structure analysis and permeability predictions for a tight gas siltstone reservoir by use of low-pressure adsorption and mercury-intrusion techniques. SPE Reservoir Evaluation & Engineering, 2012, 15(06): 648–661
33. Wu J. Study on the characteristics of coal micro-pore and its relationship with hydrocarbon migration and reservoir. Science in China, 1993, 23(1): 77–84
34. Zhang H, Yang S. Research into the nitrogen adsorption test of coal under low temperature. Journal of Shandong University of Science and Technology, 1993, 12(3): 245–249
35. Gregg S J, Sing K S W, Salzberg H W. Adsorption surface area and porosity. Journal of the Electrochemical Society, 1967, 114(11): 279C
36. Sing K S W. Reporting physisorption data for gas/solid systems with special reference to the determination of surface area and porosity. Pure and Applied Chemistry, 1985, 57(4): 603–619
37. Li X, Ma B, Xu L, Hu Z, Wang X. Thermogravimetric analysis of the co-combustion of the blends with high ash coal and waste tyres. Thermochimica Acta, 2006, 441(1): 79–83
38. Ma B G, Li X G, Xu L, Wang K, Wang X G. Investigation on catalyzed combustion of high ash coal by thermogravimetric analysis. Thermochimica Acta, 2006, 445(1): 19–22
39. Feng B, Bhatia S K, Barry J C. Variation of the crystalline structure of coal char during gasification. Energy & Fuels, 2003, 17(3): 744–754
40. Wu Y, Wu S, Gu J, Gao J. Differences in physical properties and CO_2 gasification reactivity between coal char and petroleum coke. Process Safety and Environmental Protection, 2009, 87(5): 323–330
41. Lu L, Kong C, Sahajwalla V, Harris D. Char structural ordering during pyrolysis and combustion and its influence on char reactivity. Fuel, 2002, 81(9): 1215–1225
42. Tang Z, Zhou G, Xiong J, Zhou Z. Measurement of graphitization degree of carbon-carbon composites by average X-ray diffraction angle method. The Chinese Journal of Nonferrous Metals, 2003, 13 (6): 1435–1440
43. Ding L, Gong Y, Wang Y, Wang F, Yu G. Characterisation of the morphological changes and interactions in char, slag and ash during CO_2 gasification of rice straw and lignite. Applied Energy, 2017, 195: 713–724